Tellus
SERIES B
CHEMICAL
AND PHYSICAL
METEOROLOGY
PUBLISHED BY THE INTERNATIONAL METEOROLOGICAL INSTITUTE IN STOCKHOLM

Tellus (2009), 61B, 436–448

TELLUS

Ice nuclei characteristics from M-PACE and their relation to ice formation in clouds

By ANTHONY J. PRENNI[1]*, PAUL J. DEMOTT[1], DAVID C. ROGERS[2], SONIA M. KREIDENWEIS[1], GREG M. MCFARQUHAR[3], GONG ZHANG[3] and MICHAEL R. POELLOT[4],
[1]*Department of Atmospheric Science, Colorado State University, Campus Delivery 1371, Fort Collins, CO 80523-1371, USA;* [2]*National Center for Atmospheric Research, Boulder, CO, USA;* [3]*Department of Atmospheric Sciences, University of Illinois, Urbana, IL, USA;* [4]*Department of Atmospheric Science, University of North Dakota, Grand Forks, ND, USA*

(Manuscript received 9 June 2008; in final form 15 December 2008)

ABSTRACT

This paper presents airborne measurements of ice nuclei (IN) number concentration and elemental composition from the mixed-phase Arctic cloud experiment (M-PACE) in northern Alaska during October 2004. Although the project average IN concentration was low, less than 1 L^{-1} STP, there was significant spatial and temporal variability, with local maximum concentrations of nearly 60 L^{-1} STP. Immersion and/or condensation freezing appear to be the dominant freezing mechanisms, whereas mechanisms that occur below water saturation played a smaller role. The dominant particle types identified as IN were metal oxides/dust (39%), carbonaceous particles (35%) and mixtures of metal oxides/dust with either carbonaceous components or salts/sulphates (25%), although there was significant variability in elemental composition. Trajectory analysis suggests both local and remote sources, including biomass burning and volcanic ash. Seasonal variability of IN number concentrations based on this study and data from SHEBA/FIRE-ACE indicates that fall concentrations are depleted relative to spring by about a factor of five. Average IN number concentrations from both studies compare favorably with cloud ice number concentrations of cloud particles larger than 125 μm, for temperatures less than -10°C. Cloud ice number concentrations also were enhanced in spring, by a factor of $\sim$2, but only over a limited temperature range.

1. Introduction

With growing evidence for a warming climate, a particular focus has been on the Arctic (ACIA, 2004; http://www.ipy.org/), where temperatures have risen at nearly twice the rate of the global average over the past few decades (MacBean, 2004). Greenhouse warming is amplified in the Arctic due to feedbacks involving snow and sea ice extent, the stability of the lower troposphere and thawing of permafrost (Serreze et al., 2000). Clouds also play an important role, regulating incoming solar radiation and impacting the net long-wave radiation at the surface. Although liquid water often dominates mass in Arctic stratus, the partitioning of ice and liquid water affects cloud optical depth and radiative forcing (McFarquhar and Cober, 2004; Zuidema et al., 2005; McFarquhar et al., 2007b). Cloud liquid water and ice mass content are further tied to cloud-scale dynamics, sea ice coverage and thickness and climate (Curry et al., 1996; Jiang et al., 2000; Harrington and Olsson, 2001a; Vavrus, 2004). There are also aerosol effects on Arctic clouds and climate. The first aerosol indirect effect has been shown to be of climatological importance for Arctic boundary layer clouds (Garrett and Zhao, 2006; Lubin and Vogelmann, 2006), and variations in ice nuclei (IN) concentrations have been shown to influence the liquid water content and persistence of Arctic mixed phase clouds in mesoscale model simulations (Harrington et al., 1999; Jiang et al., 2000; Prenni et al., 2007b). Thus, to quantify the extent that clouds impact Arctic climate requires knowledge of both their microphysical properties (Vavrus, 2004; Lubin and Vogelmann, 2006) and the aerosol on which they nucleate (Pinto, 1998; Harrington and Olsson, 2001b).

Low-level boundary layer clouds are prevalent in the Arctic (Curry et al., 1996; Intrieri et al., 2002; Vavrus, 2004), with liquid clouds dominating in summer, ice in winter and mixed phase in spring and autumn (Curry et al., 1997;

*Corresponding author.
e-mail: prenni@lamar.colostate.edu
DOI: 10.1111/j.1600-0889.2009.00415.x

Pinto et al., 1997; Pinto, 1998; Intrieri et al., 2002; Shupe et al., 2006). Of interest in this study are mixed phase clouds that form in spring and autumn. Arctic mixed phase clouds tend to be long lived due to a balance between cloud top radiative cooling, latent heat release, ice sedimentation and advection of moist air (Pinto, 1998; Zuidema et al., 2005). A relative scarcity of IN also favors the persistence of mixed phase clouds (Jiang et al., 2000). Arctic mixed phase clouds are characterized by liquid water content that increases with height and ice water content that decreases with height (Pinto, 1998; McFarquhar et al., 2007b). However, it is unclear if ice is generated near cloud top or cloud base (McFarquhar et al., 2007b). In some cases, entrainment of the overlying air has been correlated with increased ice production in clouds (Zuidema et al., 2005), whereas in others boundary-layer clouds appear to be more affected by aerosol from below cloud base (Hobbs and Rangno, 1998). A recent paper (Fridlind et al., 2007) suggests that on the cloud resolving model scale, it may be necessary to invoke unidentified ice formation processes to explain ice water properties.

The temperatures at which ice crystals have been observed to form (Curry et al., 1996) cover a relatively large range in lower tropospheric Arctic clouds, with liquid water sometimes reported at temperatures of -30°C and colder (Hobbs and Rangno, 1998; Intrieri et al., 2002; Verlinde et al., 2007). Primary nucleation by specific aerosol particles known as IN is thought to be responsible for initial ice formation in mixed-phase stratus clouds. Arctic IN concentrations have been measured in a number of previous studies (Bigg and Stevenson, 1970; Hobbs et al., 1971; Isono et al., 1971; Flyger et al., 1973; Jayaweera and Ohtake, 1973; Flyger et al., 1976; Radke et al., 1976; Schnell and Delany, 1976; Fountain and Ohtake, 1985; Borys, 1989; Bigg, 1996; Bigg and Leck, 2001; Rogers et al., 2001a). Although there is considerable scatter in the data among these studies, which may be due to differences in aerosol transport, instrument methods or sampling location, a key point is that most of these studies report IN concentrations of fewer than 1 L^{-1}, much lower than found at lower latitudes (Meyers et al., 1992). Some of the measurements suggest that IN concentrations can be affected by local weather (Radke et al., 1976) and local sources (Fountain and Ohtake, 1985). This may result from the persistent temperature and humidity inversions in this region, which effectively decouple the surface from the lower troposphere (Curry et al., 1996) and isolate the boundary layer from air transported higher in the atmosphere. However, several high IN episodes have been reported which correlate with long-range transport from Eurasia (Hobbs et al., 1971; Isono et al., 1971; Fountain and Ohtake, 1985; Rogers et al., 2001a).

Here, we present IN measurements from the Mixed-Phase Arctic Cloud Experiment (M-PACE) during autumn 2004. We attempt to determine possible sources for the IN measured, based on analysis of backtrajectories and IN chemical composition and number concentration. We then compare these measurements with previous measurements from this region, including measurements made during a springtime study with the same instrument used in this study. Finally, we compare average measured IN number concentrations with average measured cloud ice number concentrations using aircraft cloud particle instruments.

2. Experiment

M-PACE was conducted from late September to October 2004 in the vicinity of the DOE ARM Climate Research Facility on the North Slope of Alaska (NSA; Verlinde et al., 2007). The overall objective of the project was to collect a focused set of observations needed to advance understanding of the dynamic and microphysical processes that lead to long-lived mixed-phase Arctic clouds in fall. Measurements of cloud and aerosol properties were made by aircraft and a suite of remote sensing devices. Ice nuclei measurements were made using a Continuous Flow ice thermal Diffusion Chamber (CFDC) aboard the University of North Dakota Citation II aircraft. CFDC data were collected on 5, 6, 8, 9, 10, 16, 18, 20 and 21 October 2004.

The CFDC permits observation of ice formation on a continuous stream of aerosols at controlled temperatures and humidities (Rogers et al., 2001b). The processing section of the CFDC consists of an annular gap between two vertical, ice-coated cylinders. A laminar flow of aerosol passes through this annular space between two flows of dry, particle-free sheath air for a period of 5–10 s. The sheath flow (80%–90% of total) constrains the aerosol to a region of well-defined temperature and humidity, which is determined by the temperatures of the ice-covered walls and the location of the aerosol sample (Rogers, 1988). Particles that form ice grow preferentially due to the high supersaturations experienced by ice crystals compared with liquid particles. This size differential between ice crystals and inactivated particles is amplified prior to measuring size distributions at the outlet of the CFDC using an optical particle counter (OPC), which serves as the basis for determining IN concentrations. Amplification is due to the reduction to ice saturated conditions in the lower third of the chamber. This method allows for operation of the CFDC above water saturation, in that activated water droplets evaporate prior to reaching the OPC (Rogers, 1994). An inlet impactor upstream of the CFDC ensures that aerosol particles larger than $\sim$1.5 μm (aerodynamic diameter) are removed prior to entering the instrument (Rogers et al., 2001b), so that large aerosol particles are not erroneously identified as ice. An inertial impactor immediately downstream of the CFDC is used to capture ice crystals on Transmission Electron Microscope (TEM) grids, allowing for subsequent identification of the elemental composition of the particles on which ice forms (Kreidenweis et al., 1998). The CFDC is sensitive in real time to all nucleation modes, except contact freezing, since the residence time is fairly short.

Project average IN number concentrations from M-PACE have been reported previously (Prenni et al., 2007b). Those data were limited to observations made out-of-cloud (FSSP LWC < 0.001 g m^{-3}), as data collected while the aircraft is in-cloud may be susceptible to artefacts. Artefacts may result from large ice crystals impacting on the inlet surface, thereby shattering into fragments, generating particles from abrading the inlet and re-suspending previously deposited particles (Murphy et al., 2004). Upon further analysis, we found no clear evidence for in-cloud artefacts (e.g. no spikes in concentration or concentration gradients upon entering or exiting clouds) and no significant differences in temperature-dependent project average concentrations for in-cloud versus out-of-cloud data (95% confidence). Therefore, here we present all data collected during the study. We infer that activated IN are not excluded during cloud sampling because, they enter the inlet and then evaporate prior to reprocessing in the CFDC.

Ice nuclei number concentrations are processed and presented as 60-s running averages, and data are corrected to standard temperature and pressure (STP, 0 °C, 1 atm). Approximately 1 L of air is sampled per 60 s. Data have been processed to correct for particle losses within the CFDC (∼10%), based on laboratory tests and background counts generated through frost particle ejection from surfaces in the chamber. Filtered, particle-free air was used to establish time-dependent background concentrations throughout each flight (variable, but typically 0–2 L^{-1}). Based on these data, a simple linear regression was applied as well as time-dependent prediction intervals for background counts (at 95% confidence level). Time-dependent background corrections based on the 95% prediction interval are used throughout the paper to determine IN concentrations. For cases in which the background counts were equal to or greater than the measured IN counts, concentrations of 0 L^{-1} are reported. We note that for the low concentrations of IN measured during M-PACE, background values were often comparable to or greater than measured IN concentrations, so that 88% of the measurements were either measured as zero (∼49% of the measurements) or were less than the background concentrations (∼39% of the measurements). This means that the true IN concentrations, if very low, were not resolvable in those cases.

Atmospheric ice particle concentrations are inferred from the cloud particle instruments on the Citation for M-PACE, based on the analysis of McFarquhar et al. (2007b). These data include measurements for ice and mixed phase clouds. The primary instruments used to determine ice concentrations for this study included a particle measuring system (PMS) two-dimensional cloud particle probe (2DC; 0.03 < D < 0.96 mm) and a high volume precipitation sampler (HVPS; 0.4 < D < 40 mm). FIRE-ACE/SHEBA data are taken from Gultepe et al. (2001), with ice concentrations derived from the 2DC probe. McFarquhar et al. (2007b) and Gultepe et al. (2001) also utilized data from a Rosemount icing detector to assist in distinguishing liquid versus ice cloud regions.

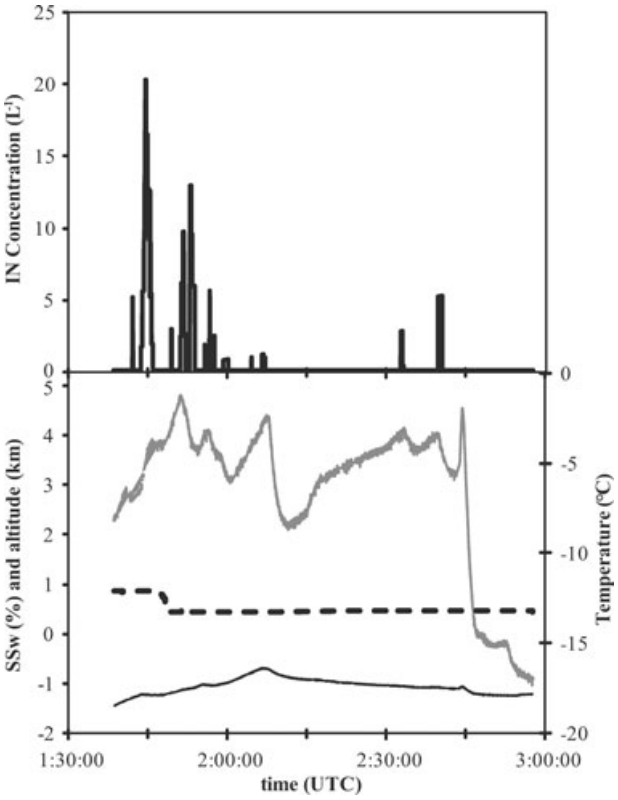

Fig. 1. Top panel: measured IN concentrations (60 s running average, STP) during the flight on 16 October 2004. Bottom panel: altitude (dashed line, left-hand axis), processing supersaturation with respect to water (SSw; thick grey line, left-hand axis) and processing temperature (thin black line, right axis) in the instrument.

3. Results and discussion

3.1. IN number concentrations

Project average IN number concentrations versus temperature were found to be low compared with lower latitudes (e.g. Meyers et al., 1992; Rogers et al., 1998; Prenni et al., 2007a; Richardson et al., 2007), in agreement with earlier studies of Arctic IN. Figure 1 shows sample data from the flight on 16 October 2004. All measurements were collected in clear air, with ambient temperatures above 0 °C for part of the flight. For most of the flight, the CFDC instrument was operated well above water saturation, so that contributions from all nucleation modes (except contact) were measured. Near the end of the flight, the humidity was dropped below water saturation to explore contributions from deposition nucleation (discussed further below). Maximum IN concentrations reached ∼20 L^{-1}, although no IN were detected for extended time intervals of the flight. This spatial inhomogeneity resulted in flight average IN concentrations of only ∼0.8 L^{-1}. This flight typified the concentrations and spatial distribution of IN during the entire project, with average values for each day shown in Fig. 2. Namely, although measured

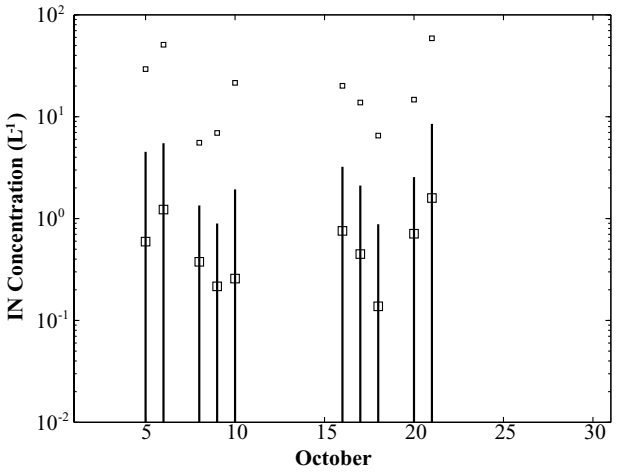

Fig. 2. Average IN concentration (STP, large squares) for each flight day, including one standard deviation of the measurement shown as error bars. Maximum IN concentrations on each day are shown as small squares.

IN concentrations reached nearly 60 L^{-1} in selected 1-min periods, project average number concentrations for all measurements were $\sim$0.7 L^{-1} due to the abundance of time periods for which no IN were present above the detection limit. We reiterate the point here, though, that aerosol particles >1.5 μm are removed prior to entering the CFDC, and so any particle larger than this cut-off size which serve as IN is not quantified in this study.

Such low IN concentrations over broad regions can impact Arctic cloud properties. For example, detailed mesoscale model simulations for a case study during M-PACE for the time period of 9–11 October showed that cloud particle phase, lifetime and radiative properties were all strongly dependent on IN concentration (Prenni et al., 2007b). Further, Prenni et al. (2007b) simulated extensive decks of liquid clouds containing smaller amounts of ice (on average) using the CFDC measurements, in reasonable agreement with observations. However, some of the high ice water contents that were observed, were not captured by the simulations. In a second study using the average measured IN number concentrations to constrain ice formation, the inability to predict the observed ice concentrations was explored (Fridlind et al., 2007). This study found that IN number concentrations would need to be more than two orders of magnitude greater than those measured to represent accurately concentrations of ice crystals larger than 53 μm that were observed in the cloud. Such high IN concentrations have only ever been observed directly in dust plumes (DeMott et al., 2003b), and so, it was hypothesized that other freezing mechanisms which cannot be captured by the CFDC or validated by any present techniques may be at play in ice-phase formation in Arctic mixed-phase stratus clouds. We provide some further elucidation of this issue in this paper.

We showed previously that IN concentration measurements during M-PACE were not a strong function of processing temperature or processing supersaturation with respect to ice (Prenni et al., 2007b). However, the data do show a dependence on processing supersaturation with respect to water (SSw; fig. 3 in Prenni et al. 2007b for the complete data set; correlation coefficient, $R = 0.83$). These data give some insight into the nucleation mechanism of the particles in the CFDC and potentially also in Arctic clouds. Observed ice nucleation in the instrument for processing conditions below water saturation is expected to occur from deposition nucleation or possibly from deliquescence freezing of haze droplets containing insoluble core particles under certain conditions (Khvorostyanov and Curry, 2005; Zobrist et al., 2008), for the temperatures explored in this study (warmer than $-30\,^{\circ}$C). Ice nucleation above water saturation occurs more readily via immersion or condensation freezing, as haze particles rapidly dilute and activate as droplets. As IN are expected to be insoluble, significant supersaturations may be needed to activate some particles as droplets and stimulate these freezing processes. At room temperature, $\sim$1% supersaturation is required for a 200 nm insoluble, wettable particle to activate as a droplet, as predicted from the Kelvin equation. We set 1% supersaturation with respect to water as a limit to crudely delineate where condensation/immersion freezing is expected to occur for most IN. Given the uncertainty in supersaturation in the CFDC, it was common to operate at a higher value than this. Thus, most data ($\sim$75%) were collected above 1% water supersaturation. Ice nuclei concentrations were more than eight times greater above this supersaturation than they were below water saturation; these means were determined to be statistically different, despite the broad variability of the measurements (*t*-test, 95% confidence). From these data, it does not appear that deposition nucleation, or any other mechanism that can occur below water saturation, played a major role in ice formation warmer than -30°C during M-PACE, and ice nucleation was dominated by condensation/immersion freezing.

Figure 3 shows project average IN data for the area covered during M-PACE. The bulk of the measurements were collected along the corridor between Barrow and Oliktok Point. The contour area approximates all areas covered throughout the study period, which in some cases is for a single flight. Most of the study area has IN concentrations of the order ≤ 1 L^{-1}, comparable to the project average, with several localized areas having IN concentrations >1 L^{-1}. One area, in particular, over the Beaufort Sea, north of Nuiqsut, stands out as having the highest IN concentrations. Positive temporal and spatial anomalies in IN concentrations have been observed previously (Pruppacher and Klett, 1997). Localized maxima may result if IN sources, such as Asian desert dust, are injected into the atmosphere and are exposed to intermittent vertical mixing and deposition, resulting in short-lived pockets of high IN concentrations far from the source (Pruppacher and Klett, 1997). Alternatively, a localized region of enhanced IN may result if there is local source.

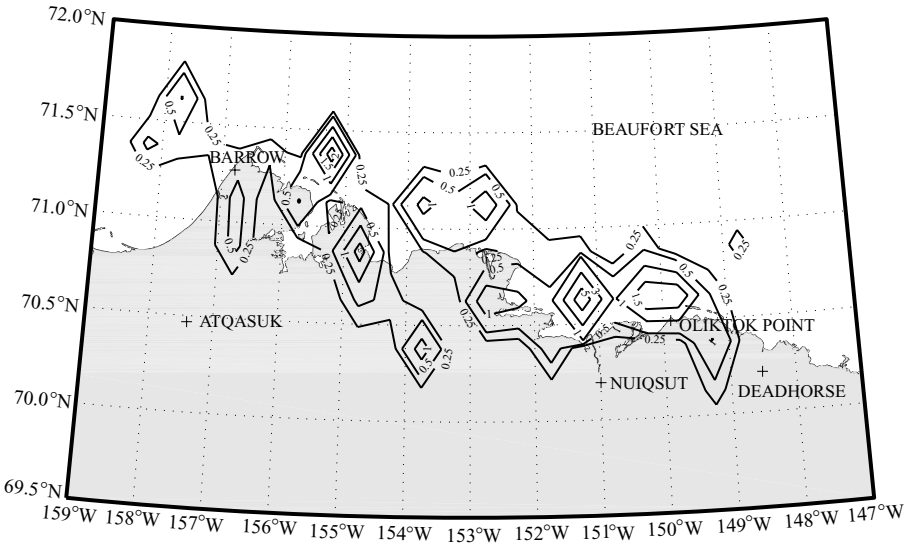

Fig. 3. Project average IN concentrations (L^{-1} STP) for the M-PACE study area, with all temperatures represented. Average IN concentrations are generally ≤ 1 L^{-1}, with a region of enhanced IN concentrations over the Beaufort Sea, centred near 70.6° N and 151.3° W. The contour area approximates the area covered during the flights.

Indeed, the location of this maximum is consistent with a possible oceanic source of IN (Bigg, 1996; Bigg and Leck, 2001; Rogers et al., 2001a). These sources are expected to come from areas free of ice, with emissions from biogenic activity (Schnell, 1977). To explore this second possibility further, we focus on the area 70.5°–71° N and 150°–152° W and consider the spatial and temporal variability of IN concentrations in this region.

During the study period, sea ice coverage expanded over the Beaufort Sea (Fetterer and Knowles, 2002, updated 2006; Verlinde et al., 2007), thus closing off potential local IN sources. As such, we consider data from the first part of the study (5–10 Oct) and the latter half (16–21 Oct) separately. Figure 4 shows average IN concentrations from this region as a function of altitude. The figure is limited to altitudes below 3200 m, where more than 85% of the data were collected. If the ocean were the source of the measured IN, we would expect an increase in IN concentrations near the surface, and we might expect a measurable decrease in IN concentrations for the latter half of the study, as sea ice coverage increased. Neither of these trends was observed. Further, for cases in which clouds were present in this region, maximum IN concentrations were observed either above cloud or within the cloud. Thus, at least during this time of the year, the measurements are not consistent with an oceanic source. This is consistent with a recent study, which suggests that Arctic marine bacteria and viruses may not be important for heterogeneous ice nucleation in the atmosphere (Junge and Swanson, 2008). However, we note that Rogers et al. (2001a) observed evidence for an oceanic IN source during spring when flying at very low altitudes over open water leads. The lack of evidence for an oceanic source from the data

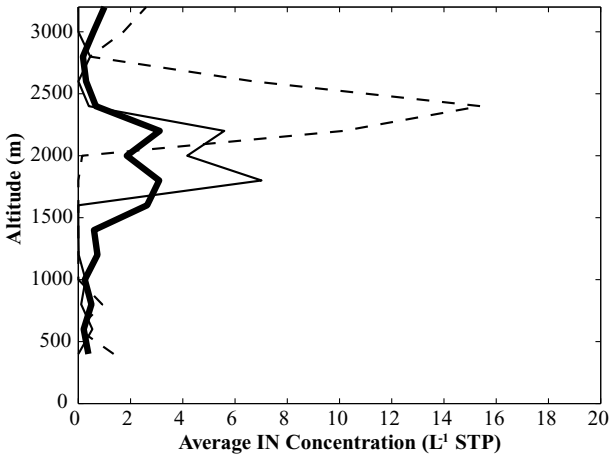

Fig. 4. IN concentration as a function of altitude. Project average data are shown for measurements near the region of maximum IN concentration shown in Fig. 3 (70.5°N–71°N and 150°W–152°W) for the first half of the project (5–10 October; thin solid line) and the second half (16–21 October; thin dashed line). The profiles represent 22–45 min of data for altitudes <1600 m and for 1600–3200 m for each time period. Project average data also are shown for the entire study area (thick solid line).

here may have occurred because we sampled regions influenced more by long-range transport from Asia (discussed below), because there may have been decreased biological activity during the colder autumnal months or because oceanic sources did not reach the altitudes sampled. Another confounding factor is that particles >1.5 μm must be removed prior to sampling in the CFDC, potentially removing IN-active bacteria.

For comparison, project average IN concentrations are shown for the entire study area in Fig. 4. Again, data collected below 3200 m represent more than 85% of the measurements. Project average IN values show a maximum above ∼1500 m, and enhanced concentrations were often observed above the boundary layer. Enhanced concentrations above the boundary layer were likely influenced by long-range transport. However, in some cases, IN concentrations were enhanced within the boundary layer; on these occasions, local and regional sources likely contributed to the measured IN.

A closer look at IN concentrations over this region shows that there were especially high values, more than 50 L^{-1}, on 2 d of the study: 6 October and 21 October. To explore possible sources of IN on these days, we use the hybrid single-particle Lagrangian integrated trajectory (HYSPLIT) model to calculate backtrajectories of the air masses that were sampled (Draxler and Rolph, 2003; Rolph, 2003). Five-day backtrajectories (FNL Meteorological data, available at http://www.arl.noaa.gov/fnl.php; Vertical motion: Model vertical velocity) were determined for each flight. This poses some difficulty for aircraft measurements since a range of latitudes, longitudes and altitudes are explored. Here, we select the point in the flight where maximum IN concentrations were measured as our starting point. For example, in Fig. 1, the maximum IN concentration was observed at 1:44:52, which corresponds to latitude 70.43°N, longitude 149.34°W and altitude 854 m. We note that running the HYSLPIT model for the range of latitudes, longitudes and altitudes encountered during the flight showed some variations, but the backtrajectories at the IN_{max} are generally representative of the airmasses sampled over most of the flight.

Results are shown in Fig. 5 and suggest that the airmass on 21 October was transported from Asia and that the airmass stayed above 2200 m for the previous 5 d (Fig. 6). We also note that there was a weak temperature inversion on this day, with maximum IN concentrations being observed well above the inversion. These observations suggest that if the IN remained aloft for more than 5 d, long-range transport was the likely source of IN on 21 October. In contrast, the airmass on 6 October (not shown) moved north through western Canada, before veering west into the Beaufort Sea. In this case, there was a stronger inversion, with maximum IN concentrations being measured very near the inversion. Further, HYSPLIT results suggest that the airmass came near the surface (∼300 m). In this case, long-range transport appears to be a less likely explanation for the enhanced concentrations; rather, boundary layer air likely provided the source of IN on 6 October. Considering data from all of the flights, the data suggest contributions from multiple sources, both local and long range, discussed further below.

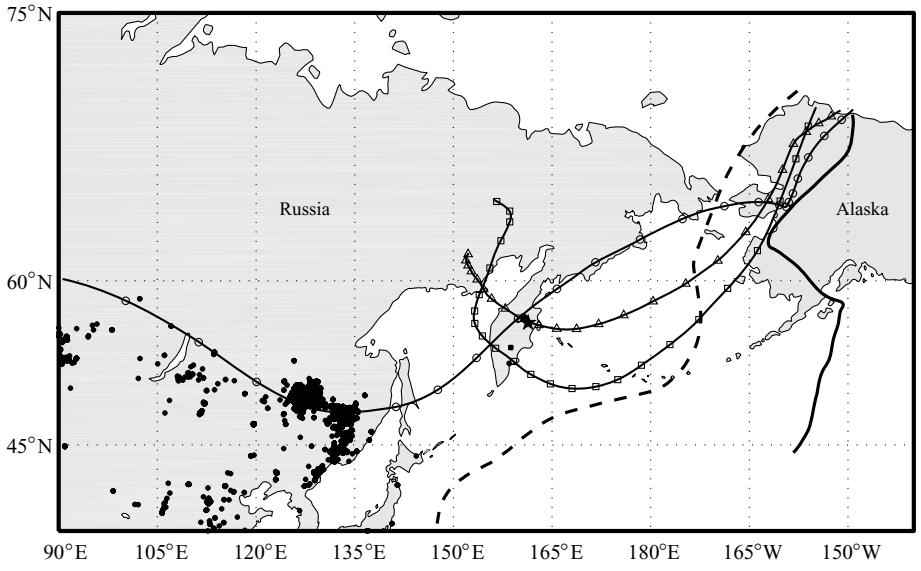

Fig. 5. Five-day backtrajectories from the sample area during five flights for which elemental composition of IN was determined from TEM analysis: 16 Oct (solid line); 17 Oct (dashed line); 18 Oct (⊖); 20 Oct (⊟) and 21 Oct (△). Symbol increments are 5 h. Also shown are fire detections based on MODIS satellite images. Except for 18 October, data are limited to hotspots observed east of 150°E for clarity. Fire detections are shown as filled symbols, with shapes corresponding to backtrajectories by date. Data are shown for fires that were detected at least 2 d prior to reaching the observation area and extending for a week beyond those 2 d. No fires were detected along the calculated backtrajectory on 16 and 17 October, numerous Asian fires and a possible contribution from an active volcano (★) were detected for the measurements on 18 October, and one fire was detected in Kamchatka for the data from 20 October. On 21 October, the calculated backtrajectory suggests that the airmass passed directly over the active Shiveluch volcano (★) in northern Kamchatka.

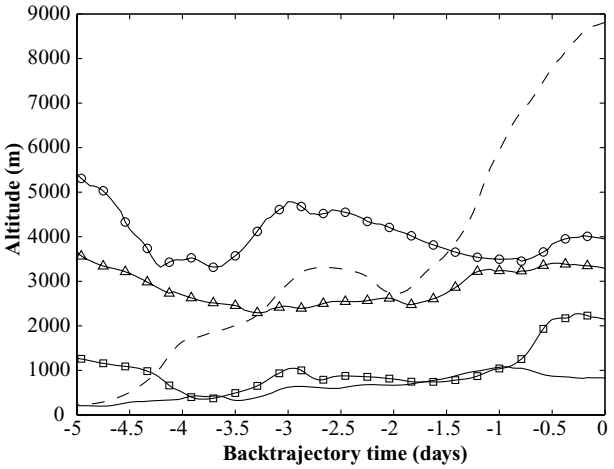

Fig. 6. Vertical component of 5 d HYSPLIT backtrajectories from Fig. 5: 16 Oct (solid line); 17 Oct (dashed line); 18 Oct (⊖); 20 Oct (⊟) and 21 Oct (⧋).

3.2. IN chemical composition

After processing in the CFDC, ice crystals were separated from aerosol particles at the outlet of the CFDC using an impactor and collected on a carbon-coated Formvar film supported by a TEM grid (Chen et al., 1998). The elemental compositions of the sampled residual nuclei were characterized using transmission electron microscopy (TEM), with energy dispersive X-ray spectroscopy (EDS). Particles were examined for IN composition on five flights: 16, 17, 18, 20 and 21 October. Data are categorized as the number fraction of analysed particles, which contain the following components: sulphates and salts; metal oxides/dust, which includes metal, metal oxide and crustal dust particles; carbonaceous particles (determined by background subtraction of carbon-coated Formvar), including soot and organic species, and mixtures of these components.

The chemical composition for the five flights includes data from ∼50 particles per flight. The size of the analysed particles, defined here as the square root of the length times the width for non-spherical particles, ranged from 30 nm to 1.29 μm, with a mean size of 0.47 μm. The dominant particle types were metal oxides/dust (39%) and carbonaceous particles (35%). Another 25% of the particles were mixtures of metal oxides/dust with either carbonaceous particles or salts/sulphates, and only 1% of the particles were pure salts/sulphates. The preponderance of metal oxides/dust as heterogeneous IN has been observed previously using the CFDC (Rogers et al., 2001a; DeMott et al., 2003a, b; Prenni et al., 2007a; Richardson et al., 2007), and early studies of the composition of Arctic IN suggested that they consist mainly of clays and related minerals (Kumai and Francis, 1962). Further, the dominant compounds observed in this category were silicon oxides (77% of metal oxide category), consistent with previous measurements of IN composition in the Arctic spring (Rogers et al., 2001a). The lack of pure salts/sulphates is expected, as homogeneous freezing was not explored in this study. There was significant day-to-day variability in chemical composition, and a variety of elements were detected: Al, Ba, C, Ca, Cl, Cr, F, Fe, K, Mg, Mn, Na, Ni, O, P, Pb, S, Se, Si, Sn, Ti and Zn. Next we explore this variability to infer potential sources of the measured IN.

HYSPLIT backtrajectories are shown for the 5 d when TEM data were collected, in Fig. 5, with the vertical component shown in Fig. 6. We reiterate the point here that the backtrajectories are for the location of the IN maximum measured on the flight. However, on each flight, the particles were collected for TEM analysis over a range of altitudes, and so, IN from both local and long-range transport sources were likely collected on the TEM grid. Therefore, for the following discussion, we consider all potential sources. Also shown in Fig. 5 are 'hotspot' detections (presumed to be fires) from MODIS during this time (Justice et al., 2002; Giglio et al., 2003; data courtesy of MODIS Rapid Response Project at NASA/GSFC and the University of Maryland). Fire emissions can be a significant source of carbonaceous particles over affected regions. Although the presence of organic compounds has been shown to be anticorrelated with ice formation in atmospheric cloud regions presumably influenced by solely heterogeneous (Targino et al., 2006) and solely homogeneous (Cziczo et al., 2004) ice nucleation, recent lidar measurements (Sassen and Khvorostyanov, 2008) and laboratory studies (M. Petters, Personal Communication, 2008) suggest that biomass burning emissions from specific types of fuel may serve effectively as heterogeneous IN. Asian biomass burning emissions can be transported from Asia to the Arctic throughout the year, with contributions from northern (>40°N) biomass burning to the Arctic reaching a maximum during summer and fall (Koch and Hansen, 2005). Except for 18 October, for clarity we have limited Asian fire detection data to fires that were observed east of 150°E. In all cases, air parcels originating from Asia took at least 3 d to reach the sampling site. Therefore, data are shown for fires that were detected at least 2 d prior to reaching the observation area and extending for a week beyond those 2 d. No fires were detected over Alaska during this time.

TEM data for each date are summarized in Table 1. On 16 October, the air that reached the sampling location came out of the south, passing through Alaska at relatively low altitudes and so was likely influenced by surface sources in the region. Metal oxides/dust and coated metal oxides and dust account for more than 80% of the particles analysed in the TEM grid. Of the metal oxides/dust, more than 95% of these particles contained silicon, consistent with an Alaskan source of wind-blown soils (Polissar et al., 1998).

The backtrajectory for the 17 October sample suggests that the air came from over the open ocean, and again particle composition was dominated by metal oxides/dust, and in particular, silicon-containing particles. Also on this date, the highest fraction of zinc-containing particles was observed (13%). A

Table 1. Summary of chemical composition of IN from five flights during M-PACE, given as the fraction of particles, by number, containing the components listed

Date	Average IN concentration (L^{-1} STP)	Metal oxides/dust	Metal oxides/dust + sulphates/salts	Metal oxides/dust + carbonaceous	Carbonaceous	Sulphates/Salts
16 October	0.76	0.65	0.02	0.15	0.19	0
17 October	0.45	0.44	0.11	0.18	0.27	0
18 October	0.14	0.22	0.08	0.20	0.50	0
20 October	0.71	0.07	0.15	0.11	0.63	0.04
21 October	1.59	0.58	0.04	0.22	0.16	0

closer look at the backtrajectory reveals that the air mass passed near to the Red Dog mining area in northwest Alaska, which is rich in surficial zinc and lead (Kelley and Hudson, 2007). Radiosonde data (http://raob.fsl.noaa.gov/) show strong surface winds at Kotzebue, ∼100 km south of Red Dog, blowing in the direction from Red Dog to the M-PACE measurement area, again suggesting a possible regional source from wind-blown soils. Of the coated metal oxides/dust particles, one contained barium and sulphur, potentially from barite, which is found in abundance naturally in the Brooks Range (Kelley and Jennings, 2004) and also is used as a weighting agent in drilling new oil wells. Additional particles containing barium and sulphur were observed on 20 and 21 October.

The backtrajectory for the 18 October sample suggests that the air passed through much of Asia, transecting regions having a large number of fires detected by MODIS. Throughout, the air parcel remained at altitudes greater than 3 km, and so, the maximum IN concentrations were likely dominated from sources due to long-range transport. The most striking changes in the data are the decrease in IN number concentration and the increase in the fraction of carbonaceous particles, with 50% of the IN containing only carbonaceous components, and another 20% mixtures of metal oxides/dust and carbonaceous components. Although fire emissions may not reach the altitudes necessary for such long-range transport, the correspondence between a sampling time in which the IN had unusually high contributions of carbonaceous material and the detection of forest fires along the backtrajectory suggest that biomass burning emissions impacted the IN measurements, and these emissions deserve further attention as potential IN. The backtrajectory also passed just west of the active Shiveluch volcano in Kamchatka. During the previous weeks, the US Geological Survey (Smithsonian Institution, 2004) reported multiple ash-and-gas explosions from Shiveluch, with ash plumes reaching several kilometres in altitude. However, the US Geological Survey (Smithsonian Institution, 2004) reported the previous week that the ash plume moved southeast of the volcano, and HYSPLIT forward trajectories indicate that the airmass originating at Shiveluch on 15 October, when the airmass passed over this region, did not transect the backtrajectory. Therefore, volcanic ash did not likely impact IN concentration or the corresponding TEM analysis on this date.

The backtrajectory for the 20 October sample again shows that the airmass passed over a fire region, this time in Kamchatka, at much lower altitudes, and again the TEM data are dominated by carbonaceous material. One of the carbonaceous particles also contained selenium, potentially from soil lofted during a convective fire.

Finally, the backtrajectory for the 21 October sample again remained at high altitudes, so that the maximum IN concentrations were likely influenced by Asian sources. In this case, the backtrajectory suggests that the air parcel passed directly over the active Shiveluch volcano in Kamchatka. On this day, the IN composition was dominated by metal oxides/dust (nearly 85%). All of these particles contained some fraction of silicon, and several contained aluminum, potassium, calcium, magnesium and/or iron, consistent with volcanic ash composition. These elements also are found in Asian dusts (Fan et al., 1996). Volcanoes previously have been identified as potential sources of IN (Isono et al., 1959a; Langer et al., 1974; Durant et al., 2008), and both maximum and average IN concentrations were enhanced on this day. These data support the notion that ash from active volcanoes can serve as a source of IN, and that long-range transport from Asia can affect IN concentrations in the Arctic.

3.3. Seasonal dependence of aerosol

An additional consideration for the Arctic is the seasonal cycle of aerosol concentration, resulting from seasonal variations in transport of aerosol from the mid-latitudes (Shaw, 1995). Indeed, previous work has shown seasonal differences in Arctic IN concentrations (Fountain and Ohtake, 1985; Bigg, 1996). Enhanced transport from mid-latitudes from about mid-December to April results in polluted 'Arctic haze', which may deactivate the ice nucleating ability of aerosol particles (Borys, 1989). However, increased aerosol transport from Asia also results in greater transport of Asian desert dusts, which serve as potential IN (Isono et al., 1959b; Sassen, 2005). Oceanic sources also are likely to have a seasonal dependence, related to variations in open water leads and biogenic activity.

Aircraft CFDC measurements of IN were made in the spring as part of FIRE-ACE/SHEBA (Rogers et al., 2001a). Here we compare M-PACE measurements with this springtime data set

Table 2. Project average composition of IN from M-PACE and SHEBA/FIRE-ACE, given as the fraction of particles, by number, containing the components listed

Project	Metal oxides/dust	Metal oxides/dust + sulphates/salts	Metal oxides/dust + carbonaceous	Carbonaceous	Sulphates/ Salts
M-PACE	0.39	0.08	0.17	0.35	0.01
SHEBA/FIRE-ACE	0.58	0.06	n/a	0.17	0.19

to determine if there are measurable seasonal differences. The springtime IN data have been re-analysed, limiting processing temperatures ($-5.7 > T > -28.5$ °C) and humidities ($5.2 > SSw > -3.2$) so that they are directly comparable with the operating conditions used during M-PACE. Data are processed as 60 s running averages at STP, using identical background corrections for equivalence with present analyses of M-PACE data. In doing this, we find that springtime IN number concentrations are enhanced relative to the measurements taken during fall by about a factor of five. The means are statistically different (*t*-test, 95% confidence), despite the broad variability of the measurements. These data suggest a seasonal dependence of IN number concentrations, which may affect cloud processes. However, it should be noted that measurements taken during M-PACE focused on the area between Prudhoe Bay and Barrow, Alaska, with most measurements occurring over land or near the coast, whereas much of the springtime data was collected over the Arctic Ocean. As such, the springtime data may have been affected by ocean sources not observed during M-PACE.

Elemental compositions of IN were determined for five flights during SHEBA/FIRE-ACE (Rogers et al., 2001a). Data are presented in Table 2 as the average elemental composition, determined from 193 particles. The TEM analysis from SHEBA/FIRE-ACE did not characterize particles that contained metal oxides/dust plus carbonaceous material. Rather, these particles are binned with the 'metal oxides/dust' category. The results are generally consistent with the trends observed during M-PACE, also shown in Table 2. Notably, the most dominant particle type was metal oxides/dust, with many of the particles containing silicon. Further, 17% of the SHEBA/FIRE-ACE IN were carbonaceous, although this value was lower than that observed during M-PACE. One difference is the enhanced fraction of particles, which contained sulphates/salts during SHEBA/FIRE-ACE. These high numbers were dominated by one TEM grid (20 May 1998), with 75% of those particles containing sulphates/salts; the reason for the enhanced values on this day is not known. Nevertheless, based on composition alone, IN sources for the spring and fall appear to be similar.

3.4. IN concentrations versus measured ice number concentrations in clouds

A composite analysis comparing measured IN concentrations to cloud-ice concentrations based on the cloud probes described above for both FIRE-ACE/SHEBA and M-PACE is shown in Fig. 7. Average IN data are shown as a function of processing temperature in the CFDC, whereas measured cloud-ice concentrations (Gultepe et al., 2001; McFarquhar et al., 2007b) are shown as a function of ambient temperature. For this figure, IN concentrations are not corrected to STP because we do not have the data necessary to do the same for the SHEBA/FIRE-ACE ice concentration data. Ice number concentrations from ice and mixed phase clouds are compared only for particles larger than 125 μm because optical probes have difficulty detecting smaller particles due to a lack of sensitivity (Strapp et al., 2001), and because even though shattering of crystals on probe inlets may produce some artefacts with $D > 125$ μm (Field et al., 2006), the majority of artefacts that are produced from shattering most likely correspond to crystals with $D < 125$ μm (Korolev and Isaac, 2005; McFarquhar et al., 2007a). For both studies, there is apparent overlap between the measured ice and measured IN number concentrations when focusing on these larger particles (correlation coefficient, $R = 0.51$ for M-PACE

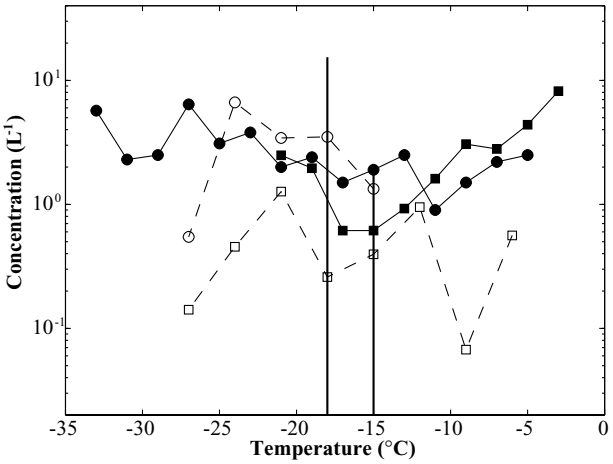

Fig. 7. Comparison between project average binned IN number concentrations (open symbols) and cloud ice number concentrations (filled symbols) from the FIRE-ACE/SHEBA project (circles; Gultepe et al., 2001) and M-PACE (squares; McFarquhar et al., 2007b) as a function of temperature, with ice crystal concentrations restricted to crystals larger than 125 μm. For comparison to the ice data, the M-PACE and FIRE-ACE/SHEBA data are not corrected to STP. The variability in the M-PACE IN measurements (one standard deviation) is shown at −15°C for this temperature, and the variability in the FIRE-ACE/SHEBA IN measurements (one standard deviation) is shown at −18°C for this temperature.

for $T = -10$ to -22 °C; $R = 0.20$ for SHEBA/FIRE-ACE for $T = -14$ to -26 °C.). Whereas Fridland et al. (2007) suggest that the measured IN from M-PACE are insufficient to predict the total ice number concentrations observed in cloud, these data suggest that ice formation processes not measured directly by the CFDC in this study (e.g. contact nucleation inside-out; Durant and Shaw, 2005) are likely linked to the measured IN concentrations.

In contrast, measured IN concentrations are two orders of magnitude lower than ice concentrations inferred from the FSSP for smaller crystals when the Rosemount icing probe indicated no measurable liquid water in clouds (Gultepe et al., 2001). We do not believe that contact freezing can explain the discrepancies because contact freezing does not likely result from a source of IN that is independent of the source of condensation/immersion freezing nuclei (Durant and Shaw, 2005). However, there is potential to overestimate particle concentrations with the FSSP and similar probes in the presence of ice (Gardiner and Hallett, 1985; Field et al., 2003; Field et al., 2006; McFarquhar et al., 2007a). Additional measurements and modelling studies are needed to fully explain the discrepancies between IN and ice number concentrations for these smaller cloud particles. It is also interesting to note that cloud ice number concentrations are enhanced in spring by about a factor of two compared with autumn for temperatures less than -10 °C, in qualitative agreement with the IN measurements. At higher temperatures (> -10 °C), ice number concentrations in cloud are enhanced relative to the measured IN. The enhanced ice number concentrations correlate with a decrease in the liquid mass fraction in these clouds over this temperature range (McFarquhar et al., 2007b) and may result from ice multiplication processes (Hobbs and Rangno, 1998; Rangno and Hobbs, 2001).

4. Summary and conclusions

The M-PACE field study was conducted in the fall of 2004 near the DOE North Slope of Alaska field site. Airborne measurements of IN were obtained using the CFDC method. The IN data are presented as measured number concentrations and chemical compositions of IN. Measured IN concentrations were variable, with concentrations ranging from 0–60 L^{-1} at STP. However, due to the abundance of measurements for which IN concentrations fell below the detection limit of the instrument, the project average number concentration was less than 1 L^{-1} STP for the broad range of temperatures (-6 to -28 °C) and humidities explored. Such low concentrations of IN are in agreement with previous studies and are qualitatively consistent with the existence of large regions of liquid and mixed phase clouds in the Arctic in autumn. Of the IN measured, immersion and condensation freezing appear to be the dominant freezing mechanisms, whereas deposition freezing, or any other mechanism that may occur below water saturation, played a much smaller role. Contact freezing could not be assessed, but assuming that contact freezing nuclei come from the same particles types as condensation freezing nuclei, contact freezing nuclei concentrations also are likely to be quite low.

These data were compared with CFDC measurements made in spring during SHEBA/FIRE-ACE. Springtime IN concentrations were enhanced relative to the measurements taken during fall by about a factor of five. Such seasonal variability of IN may be expected due to differences in transport of aerosol from the mid-latitudes during spring and fall and due to the fact that local sources may be suppressed when the surface is snow and ice covered. Seasonal differences in IN concentration may affect cloud processes. Indeed, measurements of ice in clouds from the two studies show cloud ice number concentrations enhanced in spring compared with autumn.

Ice nuclei sources have been inferred from elemental analysis of measured IN, spatial distribution of IN concentrations and HYSPLIT backtrajectory analysis of the airmasses that were encountered during the flights. These measurements include air from both within and above the boundary layer, and the data suggest multiple sources of IN to this region, including aerosol from local and long-range transport. Dominant particle types were metal oxides/dust, carbonaceous particles and mixtures of metal oxides/dust with either carbonaceous particles or salts/sulphates, with significant day-to-day variability. Variability in composition was related to potential local sources and the backtrajectories of the particles. In particular, measurements of IN residuals from samples, which were thought to have passed over regions of Asian biomass burning, showed that a large fraction of the IN were carbonaceous, whereas compositions indicative of volcanic ash correlated with a backtrajectory that passed very near an active volcano. Elemental compositions from M-PACE were consistent with elemental IN composition determined in spring during SHEBA/FIRE-ACE.

For both M-PACE and SHEBA/FIRE-ACE, project average IN number concentrations showed good agreement with cloud ice number concentrations for cloud particles with maximum dimensions larger than 125 μm and for temperatures colder than about -10 °C. We note that although IN and ice concentration data were not cosampled, it provides anecdotal evidence that should stimulate future modelling and observational studies. This agreement also suggests that these larger ice particles likely formed from primary nucleation. At warmer temperatures, cloud ice number concentrations exceeded measured IN, indicative of secondary ice formation processes active in this temperature range. Measured IN concentrations were significantly lower than cloud ice, when smaller ice crystals were included in the analysis. This is consistent with previous comparisons of IN measured using the CFDC and cloud ice measured using the FSSP (Prenni et al., 2007a) and may be tied to the observation that particle concentrations may be overestimated with the FSSP in the presence of ice (Gardiner and Hallett, 1985; Field et al., 2003, 2006; McFarquhar et al., 2007a).

5. Acknowledgments

A.J.P. and P.J.D. were supported by the Office of Biological and Environmental Research of the US Department of Energy (under grant DE-FG02-06ER64176) as part of the Atmospheric Radiation Measurement Program. SHEBA/FIRE-ACE measurements were supported by NASA grants NAG-2-924 and NAG-1-2063. The authors gratefully acknowledge the NOAA Air Resources Laboratory (ARL) for the provision of the HYSPLIT transport and dispersion model and/or READY website (http://www.arl.noaa.gov/ready.html) used in this publication. Fire data courtesy of MODIS Rapid Response Project at NASA/GSFC and the University of Maryland.

References

ACIA. 2004. *Impacts of a Warming Arctic: Arctic Climate Impact Assessment*. Cambridge University Press, Cambridge. Available at: http://www.acia.uaf.edu.

Bigg, E. K. 1996. Ice forming nuclei in the high Arctic. *Tellus B* **48**, 223–233.

Bigg, E. K. and Leck, C. 2001. Cloud-active particles over the central Arctic Ocean. *J. Geophys. Res. (Atmos.)* **106**, 32 155–32 166.

Bigg, E. K. and Stevenson, M. 1970. Comparison of concentrations of ice nuclei in different parts of the world. *J. Rech. Atmos.* **4**, 41–58.

Borys, R. D. 1989. Studies of ice nucleation by Arctic aerosol on AGASP-II. *J. Atmos. Chem.* **9**, 169–185.

Chen, Y., Kreidenweis, S. M., McInnes, L. M., Rogers, D. C. and DeMott, P. J. 1998. Single particle analyses of ice nucleating aerosols in the upper troposphere and lower stratosphere. *Geophys. Res. Lett.* **25**, 1391–1394.

Curry, J. A., Rossow, W. B., Randall, D. and Schramm, J. L. 1996. Overview of Arctic cloud and radiation characteristics. *J. Clim.* **9**, 1731–1764.

Curry, J. A., Pinto, J. O., Benner, T. and Tschudi, M. 1997. Evolution of the cloudy boundary layer during the autumnal freezing of the Beaufort Sea. *J. Geophys. Res. (Atmos.)* **102**, 13 851–13 860.

Cziczo, D. J., DeMott, P. J., Brooks, S. D., Prenni, A. J., Thomson, D. S. and co-authors. 2004. Observations of organic species and atmospheric ice formation. *Geophys. Res. Lett.* **31**, L12116, doi:12110.11029/12004GL019822.

DeMott, P. J., Cziczo, D. J., Prenni, A. J., Murphy, D. M., Kreidenweis, S. M. and co-authors. 2003a. Measurements of the concentration and composition of nuclei for cirrus formation. *P. Natl. Acad. Sci. USA* **100**, 14 655–14 660.

DeMott, P. J., Sassen, K., Poellot, M. R., Baumgardner, D., Rogers, D. C. and co-authors. 2003b. African dust aerosols as atmospheric ice nuclei. *Geophys. Res. Lett.* **30**, Art. No. 1732, doi:10.1029/2003GL071410.

Draxler, R. R. and Rolph, G. D. 2003. HYSPLIT (hybrid single-particle lagrangian integrated trajectory) Model, NOAA Air Resources Laboratory, Silver Spring, MD. Available at: http://www.arl.noaa.gov/ready/hysplit4.html (NOAA ARL READY Website).

Durant, A. J. and Shaw, R. A. 2005. Evaporation freezing by contact nucleation inside-out. *Geophys. Res. Lett.* **32**, Art. No. L20814, doi:10.1029/2005GL024175.

Durant, A. J., Shaw, R. A., Rose, W. I., Mi, Y. and Ernst, G. G. J. 2008. Ice nucleation and overseeding of ice in volcanic clouds. *J. Geophys. Res. (Atmos.)* **113**, doi:10.1029/2007JD009064.

Fan, X. B., Okada, K., Niimura, N., Kai, K., Arao, K. and co-authors. 1996. Mineral particles collected in China and Japan during the same Asian dust-storm event. *Atmos. Environ.* **30**, 347–351.

Fetterer, F. and Knowles, K. 2002 (Updated 2006). *Sea Ice Index*. National Snow and Ice Data Center, Boulder, CO.

Field, P. R., Wood, R., Brown, P. R. A., Kaye, P. H., Hirst, E. and co-authors. 2003. Ice particle interarrival times measured with a fast FSSP. *J. Atmos. Ocean. Tech.* **20**, 249–261.

Field, P. R., Heymsfield, A. J. and Bansemer, A. 2006. Shattering and particle interarrival times measured by optical array probes in ice clouds. *J. Atmos. Ocean. Tech.* **23**, 1357–1371.

Flyger, H., Hansen, K., Megaw, W. J. and Cox, L. C. 1973. The background level of the summer tropospheric aerosol over Greenland and the North Atlantic Ocean. *J. Appl. Meteorol.* **12**, 161–174.

Flyger, H., Heidam, N. Z., Hansen, K., Megaw, W. J., Walther, E. G. and co-authors. 1976. The background level of the summer tropospheric aerosol, sulfur dioxide and ozone over Greenland and the North Atlantic Ocean. *J. Aerosol Sci.* **7**, 103–140.

Fountain, A. G. and Ohtake, T. 1985. Concentrations and source areas of ice nuclei in the Alaskan atmosphere. *J. Clim. Appl. Meteorol.* **24**, 377–382.

Fridlind, A. M., Ackerman, A. S., McFarquhar, G., Zhang, G., Poellot, M. R. and co-authors. 2007. Ice properties of single-layer stratocumulus during the Mixed-Phase Arctic Cloud Experiment (M-PACE), 2: model results. *J. Geophys. Res. (Atmos.)* **112**, doi:10.1029/2007JD008646.

Gardiner, B. A. and Hallett, J. 1985. Degradation of in-cloud forward scattering spectrometer probe measurements in the presence of ice particles. *J. Atmos. Ocean. Tech.* **2**, 171–180.

Garrett, T. J. and Zhao, C. F. 2006. Increased Arctic cloud longwave emissivity associated with pollution from mid-latitudes. *Nature* **440**, 787–789.

Giglio, L., Descloitres, J., Justice, C. O. and Kaufman, Y. J. 2003. An enhanced contextual fire detection algorithm for MODIS. *Remote Sens. Environ.* **87**, 273–282.

Gultepe, I., Isaac, G. A. and Cober, S. G. 2001. Ice crystal number concentration versus temperature for climate studies. *Int. J. Climatol.* **21**, 1281–1302.

Harrington, J. Y. and Olsson, P. Q. 2001a. A method for the parameterization of cloud optical properties in bulk and bin microphysical models: implications for arctic cloudy boundary layers. *Atmos. Res.* **57**, 51–80.

Harrington, J. Y. and Olsson, P. Q. 2001b. On the potential influence of ice nuclei on surface-forced marine stratocumulus cloud dynamics. *J. Geophys. Res. (Atmos.)* **106**, 27 473–27 484.

Harrington, J. Y., Reisin, T., Cotton, W. R. and Kreidenweis, S. M. 1999. Cloud resolving simulations of Arctic stratus, part II: transition-season clouds. *Atmos. Res.* **51**, 45–75.

Hobbs, P. V. and Rangno, A. L. 1998. Microstructures of low and middle-level clouds over the Beaufort Sea. *Q. J. Roy. Meteor. Soc.* **124**, 2035–2071.

Hobbs, P. V., Bluhm, G. C. and Ohtake, T. 1971. Transport of ice nuclei over North Pacific Ocean. *Tellus* **23**, 28–39.

Intrieri, J. M., Shupe, M. D., Uttal, T. and McCarty, B. J. 2002. An annual cycle of Arctic cloud characteristics observed by radar and lidar at SHEBA. *J. Geophys. Res.—Oceans* **107**, Article Number 8030, doi:10.1029/2000JC000439.

Isono, K., Komabayasi, M. and Ono, A. 1959a. Volcanoes as a source of atmospheric ice nuclei. *Nature* **183**, 317–318.

Isono, K., Komabayasi, M. and Ono, A. 1959b. The nature and origin of ice nuclei in the atmosphere. *J. Meteorol. Soc. Jpn.* **37**, 211–233.

Isono, K., Komabayasi, M., Takeda, T., Tanaka, T., Iwai, K. and co-authors. 1971. Concentration and nature of ice nuclei in rim of the North Pacific Ocean. *Tellus* **23**, 40–58.

Jayaweera, K. O. L. F. and Ohtake, T. 1973. Concentrations of ice crystals in Arctic stratus clouds. *J. Rech. Atmos.* **7**, 199–207.

Jiang, H. L., Cotton, W. R., Pinto, J. O., Curry, J. A. and Weissbluth, M. J. 2000. Cloud resolving simulations of mixed-phase Arctic stratus observed during BASE: sensitivity to concentration of ice crystals and large-scale heat and moisture advection. *J. Atmos. Sci.* **57**, 2105–2117.

Junge, K. and Swanson, B. D. 2008. High-resolution ice nucleation spectra of sea-ice bacteria: implications for cloud formation and life in frozen environments. *Biogeosciences* **5**, 865–873.

Justice, C. O., Giglio, L., Korontzi, S., Owens, J., Morisette, J. T. and co-authors. 2002. The MODIS fire products. *Remote Sens. Environ.* **83**, 244–262.

Kelley, K. D. and Hudson, T. 2007. Natural versus anthropogenic dispersion of metals to the environment in the Wulik River area, western Brooks Range, northern Alaska. *Geochem.-Explor. Env. A.* **7**, 87–96.

Kelley, K. D. and Jennings, S. 2004. A special issue devoted to barite and Zn-Pb-Ag deposits in the Red Dog district, Western Brooks Range, Northern Alaska. *Econ. Geol.* **99**, 1267–1280.

Khvorostyanov, V. I. and Curry, J. A. 2005. The theory of ice nucleation by heterogeneous freezing of deliquescent mixed CCN, part II: parcel model simulation. *J. Atmos. Sci.* **62**, 261–285.

Koch, D. and Hansen, J. 2005. Distant origins of Arctic black carbon: a Goddard Institute for Space Studies Model Eexperiment. *J. Geophys. Res. (Atmos.)* **110**, Art. No. D04204, doi:10.1029/2004JD005296.

Korolev, A. and Isaac, G. A. 2005. Shattering during sampling by OAPs and HVPS, part 1: snow particles. *J. Atmos. Ocean. Tech.* **22**, 528–542.

Kreidenweis, S. M., Chen, Y., Rogers, D. C. and DeMott, P. J. 1998. Isolating and identifying atmospheric ice-nucleating aerosols: a new technique. *Atmos. Res.* **46**, 263–278.

Kumai, M. and Francis, K. E. 1962. Nuclei in snow and ice crystals on the Greenland Ice Cap under natural and artificially stimulated conditions. *J. Atmos. Sci.* **19**, 474–481.

Langer, G., Garcia, C. J., Mendonca, B. G., Pueschel, R. F. and Fullerto, Cm. 1974. Hawaiian volcanos—source of ice nuclei. *J. Geophys. Res.* **79**, 873–875.

Lubin, D. and Vogelmann, A. M. 2006. A climatologically significant aerosol longwave indirect effect in the Arctic. *Nature* **439**, 453–456.

MacBean, G. 2004. Arctic climate—past and present. In: *Impacts of a Warming Arctic: Arctic Climate Impacts Assessment* (ed. S. J. Hassol). Cambridge University Press, New York, 21–60. Available at http://www.acia.uaf.edu.

McFarquhar, G. M. and Cober, S. G. 2004. Single-scattering properties of mixed-phase Arctic clouds at solar wavelengths: impacts on radiative transfer. *J. Clim.* **17**, 3799–3813.

McFarquhar, G. M., Um, J., Freer, M., Baumgardner, D., Kok, G. L. and co-authors. 2007a. Importance of small ice crystals to cirrus properties: observations from the Tropical Warm Pool International Cloud Experiment (TWP-ICE). *Geophys. Res. Lett.* **34**, L13803.

McFarquhar, G. M., Zhang, G., Poellot, M. R., Kok, G. L., McCoy, R. and co-authors. 2007b. Ice properties of single layer stratocumulus during the Mixed-Phase Arctic Cloud Experiment (M-PACE), part 1: observations. *J. Geophys. Res. (Atmos.)* **112**, doi:10.1029/2007JD008633.

Meyers, M. P., Demott, P. J. and Cotton, W. R. 1992. New primary ice-nucleation parameterizations in an explicit cloud model. *J. Appl. Meteorol.* **31**, 708–721.

Murphy, D. M., Cziczo, D. J., Hudson, P. K., Thomson, D. S., Wilson, J. C. and co-authors. 2004. Particle generation and resuspension in aircraft inlets when flying in clouds. *Aerosol Sci. Tech.* **38**, 400–408.

Pinto, J. O. 1998. Autumnal mixed-phase cloudy boundary layers in the Arctic. *J. Atmos. Sci.* **55**, 2016–2038.

Pinto, J. O., Curry, J. A. and Fairall, C. W. 1997. Radiative characteristics of the Arctic atmosphere during spring as inferred from ground-based measurements. *J. Geophys. Res. (Atmos.)* **102**, 6941–6952.

Polissar, A. V., Hopke, P. K., Malm, W. C. and Sisler, J. F. 1998. Atmospheric aerosol over Alaska, 1: spatial and seasonal variability. *J. Geophys. Res. (Atmos.)* **103**, 19 035–19 044.

Prenni, A. J., DeMott, P. J., Twohy, C., Poellot, M. R., Kreidenweis, S. M. and co-authors. 2007a. Examinations of ice formation processes in Florida cumuli using ice nuclei measurements of anvil ice crystal particle residues. *J. Geophys. Res. (Atmos.)* **112**, Art. No. D10221, doi:10.1029/2006JD007549.

Prenni, A. J., Harrington, J. Y., Tjernström, M., DeMott, P. J., Avramov, A., and co-authors. 2007b. Can ice-nucleating aerosols affect Arctic seasonal climate? *Bull. Am. Meteorol. Soc.* **88**, 541–550.

Pruppacher, H. R. and Klett, J. D. 1997. *Microphysics of Clouds and Precipitation*. Kluwer Academic Publishers, Dordrecht, The Netherlands.

Radke, L. F., Hobbs, P. V. and Pinnons, J. E. 1976. Observations of cloud condensation nuclei, sodium-containing particles, ice nuclei and light-scattering coefficient near Barrow, Alaska. *J. Appl. Meteorol.* **15**, 982–995.

Rangno, A. L. and Hobbs, P. V. 2001. Ice particles in stratiform clouds in the Arctic and possible mechanisms for the production of high ice concentrations. *J. Geophys. Res. (Atmos.)* **106**, 15 065–15 075.

Richardson, M. S., DeMott, P. J., Kreidenweis, S. M., Cziczo, D. J., Dunlea, E. J. and co-authors. 2007. Measurements of heterogeneous ice nuclei in the western United States in springtime and their relation to aerosol characteristics. *J. Geophys. Res (Atmos.)* **112**, D02209.

Rogers, D. C. 1988. Development of a continuous flow thermal gradient diffusion chamber for ice nucleation studies. *Atmos. Res.* **22**, 149–181.

Rogers, D. C. 1994. Detecting ice nuclei with a continuous-flow diffusion chamber—some exploratory tests of instrument response. *J. Atmos. Ocean. Tech.* **11**, 1042–1047.

Rogers, D. C., DeMott, P. J., Kreidenweis, S. M. and Chen, Y. L. 1998. Measurements of ice nucleating aerosols during SUCCESS. *Geophys. Res. Lett.* **25**, 1383–1386.

Rogers, D. C., DeMott, P. J. and Kreidenweis, S. M. 2001a. Airborne measurements of tropospheric ice-nucleating aerosol particles in the Arctic spring. *J. Geophys. Res. (Atmos.)* **106**, 15 053–15 063.

Rogers, D. C., DeMott, P. J., Kreidenweis, S. M. and Chen, Y. 2001b. A continuous-flow diffusion chamber for airborne measurements of ice nuclei. *J. Atmos. Ocean. Tech.* **18**, 725–741.

Rolph, G. D. 2003. Real-time environmental applications and display system (READY). NOAA Air Resources Laboratory, Silver Spring, MD. Available at http://www.arl.noaa.gov/ready/hysplit4.html.

Sassen, K. 2005. Dusty ice clouds over Alaska. *Nature* **434**, 456–456.

Sassen, K. and Khvorostyanov, V. I. 2008. Cloud effects from boreal forest fire smoke: evidence for ice nucleation from polarization lidar data and cloud model simulations. *Environ. Res. Lett.* **3**, doi:10.1088/1748-9326/1083/1082/025006.

Schnell, R. C. 1977. Ice nuclei in seawater, fog water and marine air off coast of Nova-Scotia—summer 1975. *J. Atmos. Sci.* **34**, 1299–1305.

Schnell, R. C. and Delany, A. C. 1976. Airborne ice nuclei near an active volcano. *Nature* **264**, 535–536.

Serreze, M. C., Walsh, J. E., Chapin, F. S., Osterkamp, T., Dyurgerov, M. and co-authors. 2000. Observational evidence of recent change in the northern high-latitude environment. *Clim. Change* **46**, 159–207.

Shaw, G. E. 1995. The arctic haze phenomenon. *Bull. Am. Meteorol. Soc.* **76**, 2403–2413.

Shupe, M. D., Matrosov, S. Y. and Uttal, T. 2006. Arctic mixed-phase cloud properties derived from surface-based sensors at SHEBA. *J. Atmos. Sci.* **63**, 697–711.

Smithsonian Institution. 2004. *US Geological Survey Weekly Volcanic Activity Report*. Kamchatkan Volcanic Eruption Response Team, Global Volcanism Program.

Strapp, J. W., Albers, F., Reuter, A., Korolev, A. V., Maixner, U. and co-authors. 2001. Laboratory measurements of the response of a PMS OAP-2DC. *J. Atmos. Ocean. Tech.* **18**, 1150–1170.

Targino, A. C., Krejci, R., Noone, K. J. and Glantz, P. 2006. Single particle analysis of ice crystal residuals observed in orographic wave clouds over Scandinavia during INTACC experiment. *Atmos. Chem. Phys.* **6**, 1977–1990.

Vavrus, S. 2004. The impact of cloud feedbacks on Arctic climate under greenhouse forcing. *J. Climate* **17**, 603–615.

Verlinde, J., Harrington, J. Y., McFarquhar, G. M., Yannuzzi, V. T., Avramov, A. and co-authors. 2007. The mixed-phase Arctic cloud experiment. *Bull. Am. Meteorol. Soc.* **88**, 205–221.

Zobrist, B., Marcolli, C., Peter, T. and Koop, T. 2008. Heterogeneous ice nucleation in aqueous solutions: the role of water activity. *J. Phys. Chem. A* **112**, 3965–3975.

Zuidema, P., Baker, B., Han, Y., Intrieri, J., Key, J. and co-authors. 2005. An Arctic springtime mixed-phase cloudy boundary layer observed during SHEBA. *J. Atmos. Sci.* **62**, 160–176.